

Structural and Compositional Investigations on Stability of Cuprous Oxide Nanowire Photocathodes for Photoelectrochemical Water Splitting

Min-Kyu Son^{1*}, Linfeng Pan², Matthew T. Mayer³, Anders Hagfeldt², Michael Grätzel⁴ and Jingshan Luo^{5*}

¹Nanomaterials and Nanotechnology Center, Electronic Convergence Division, Korea Institute of Ceramic Engineering & Technology (KICET), Jinju 52851, Republic of Korea

²Laboratory of Photomolecular Science, Institute of Chemical Sciences and Engineering, École Polytechnique Fédérale de Lausanne (EPFL), Lausanne, CH-1015 Switzerland

³Helmholtz-Zentrum Berlin für Materialien und Energie, 14109 Berlin, Germany

⁴Laboratory of Photonics and Interfaces, Institute of Chemical Sciences and Engineering, École Polytechnique Fédérale de Lausanne (EPFL), Lausanne, CH-1015 Switzerland

⁵Institute of Photoelectronic Thin Film Devices and Technology, Key Laboratory of Photoelectronic Thin Film Devices and Technology of Tianjin, Ministry of Education Engineering Research Center of Thin Film Photoelectronic Technology, Renewable Energy Conversion and Storage Center, Nankai University, Tianjin 300350, China

*E-mail: minkyu.son@kicet.re.kr ; jingshan.luo@nankai.edu.cn

ABSTRACT

Cuprous oxide (Cu₂O) is a promising photocathode material for photoelectrochemical (PEC) water splitting. Recently, the PEC performances of Cu₂O-based devices have been considerably improved by introducing nanostructures, semiconductor overlayers and hydrogen evolution reaction (HER) catalysts. However, Cu₂O devices still suffer from poor stability in aqueous solution, especially in strong acidic or alkaline conditions, despite the use of an intrinsically stable oxide overlayer as a protection layer. Thus, it is essential to fully understand the stability of the entire Cu₂O photocathodes in these conditions for establishing suitable protection strategies to achieve durable PEC water splitting. In this work, the stability of bare and protected Cu₂O nanowire (NW) photocathodes were evaluated in detail using microscopy techniques and compositional analyses. The insights gained in this work will guide the design and synthesis of durable photoelectrodes for PEC water splitting.

KEYWORDS: Cuprous oxide, Nanowire structure, Photocathode, Photoelectrochemical water splitting, Stability

Cuprous oxide (Cu_2O) has been intensively investigated as a promising photocathode material for photoelectrochemical (PEC) water splitting to generate hydrogen because it has p-type characteristics and a favorable conduction band position for hydrogen evolution with a band gap of ~ 2 eV, which is responsive to visible light.¹⁻³ Furthermore, it is an earth-abundant material with low toxicity, thereby enabling eco-friendly hydrogen generation at low cost.^{4,5} With many efforts from several groups, the PEC performance of Cu_2O photocathodes has been successfully improved by introducing oxide under/overlayers^{2,3,6-9} and various hydrogen evolution reaction (HER) catalysts.^{2,3,10,11} Recently, we have enhanced the PEC performance of Cu_2O photocathodes using nanowire (NW) structures.^{12,13} High quality Cu_2O NW structures showed better light absorption and charge collection, compared to the planar Cu_2O film. Hence, its photocurrent density reached 10 mA cm^{-2} biased at the thermodynamic hydrogen evolution potential in pH 5 electrolyte.¹³

Despite such considerable performance improvement, Cu_2O photocathodes still face a big challenge for real PEC water splitting application due to its poor stability.^{1,2,14,15} In general, the p-type semiconductor is stable for HER when its reduction potential is more negative than the hydrogen evolution potential.¹⁶ However, Cu_2O does not meet this criterion because its reduction potential is lower (more positive) than the hydrogen evolution potential. On the other hand, its oxidation potential is higher (less positive) than the oxygen evolution potential. Therefore, Cu_2O can be easily oxidized to cupric oxide (CuO) or reduced to metallic copper (Cu) when it is directly in contact with electrolyte for PEC water splitting.^{1,17-19} To prevent this, various strategies have been introduced. The most common one is to use intrinsically stable oxides such as titanium oxide (TiO_2)^{1,2} and tin oxide (SnO_2)²⁰ as protection layers. The Cu_2O photocathodes with these protection layers showed a stable PEC performance in the near-neutral pH solution for many hours. It has also been demonstrated that some post treatments such as low temperature steam annealing²¹ or surface etching modification¹⁸ are effective to enhance the stability of Cu_2O photocathodes. Although these strategies have successfully alleviated the degradation of Cu_2O photocathodes, it is still not enough for practical PEC water splitting operation, which demands stability for many years. Therefore, it is necessary to understand the stability of Cu_2O photocathodes during the PEC water splitting process for establishing suitable and effective protection strategies.

There have been some studies on the stability of Cu_2O in aqueous solution. For example, Wu et al. found that the morphology of the electrodeposited Cu_2O film changed without any compositional difference due to the recrystallization process when it is soaked in aqueous solution.¹⁷ Sowers et al. reported that the crystal face of Cu_2O influences the deterioration of Cu_2O photocathodes in water.²² It was also reported that the (100) facet of Cu_2O was less stable than other facets, resulting in faster degradation.^{23,24} However, these studies did not give sufficient insights into the stability of the entire Cu_2O photocathode for PEC water splitting because they only focused on the stability of bare Cu_2O . The state-of-the-art Cu_2O photocathodes consist of an n-type semiconductor overlayer for enhanced charge separation, a protection layer and the HER catalyst, as well as the Cu_2O film. Although these components could also contribute to the stability of Cu_2O photocathodes during PEC operation, their influences on stability have not been studied to date.

In addition, the introduction of NW structure photoelectrode and operation in extreme pH

solutions (acidic or alkaline solutions) for enhanced PEC performances would make the degradation process of Cu₂O photocathodes more complicated compared to the classical ones (planar structure and operation in near-neutral solution). The NW structure photoelectrode provides enhanced light absorption and improved charge collection, thus resulting in improved PEC performances.^{12,25} On the other hand, high surface area electrodes offer more possibility for degradation. Moreover, although it is desirable to operate water splitting photoelectrodes in a neutral solution such as seawater for practical PEC water splitting, the operation in extreme alkaline or acidic solutions is also significant to minimize pH gradients and cell resistance.^{26,27} However, the Cu₂O photocathode is vulnerable to corrosion under such conditions according to its Pourbaix diagram.²⁸ These aspects should be considered for understanding the stability of the entire Cu₂O photocathode.

In this work, the stability of Cu₂O photocathodes was comprehensively studied during the PEC water splitting process using Cu₂O NW photocathodes with Al:ZnO (AZO) overlayer, TiO₂ protection layer and ruthenium oxide (RuO_x) HER catalyst. First, the electrochemical reactions and their influences on stability of bare Cu₂O NW photocathodes in the neutral aqueous solution were investigated. Second, the stability of Cu₂O NW photocathodes with AZO/TiO₂ overlayers and HER catalyst in the neutral aqueous solution was investigated, focusing on the catalyst influence. Third, the chemical and PEC stability of Cu₂O NW photocathodes with AZO/TiO₂ overlayers and RuO_x HER catalyst in acidic/alkaline aqueous solutions was examined. Finally, the effect of thermal treatments on the crystallization of the amorphous TiO₂ protection layer for further improving the stability and its effect on Cu₂O NW photocathodes were also investigated. Based on these studies, we proposed feasible strategies for developing efficient and durable Cu₂O photocathodes for solar water splitting in the conclusion section.

RESULTS AND DISCUSSION

Stability of Bare Cu₂O NW Photocathodes. It is well-known that Cu₂O photocathodes without overlayers and protection layer are quite unstable even in the aqueous solution with mild pH conditions.^{1,2} In general, Cu₂O can be changed into the metallic Cu with the reduction reaction (Reaction 1). Furthermore, it can also be converted into CuO or copper hydroxide (Cu(OH)₂) with the oxidation reactions (Reaction 2 or 3), described below.

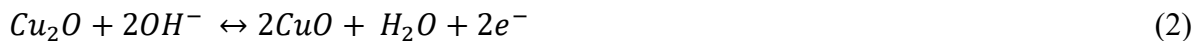


Figure 1a shows redox reaction potential windows of Cu₂O, converted to the reversible hydrogen electrode (RHE) scale from literatures.^{1,17, 29-31} Cu₂O can be reduced to the metallic Cu in the potential windows of 0.3-0.45 V versus RHE, while it can be oxidized to CuO and Cu(OH)₂ in the potential windows of 0.6-0.85 V and 0.75-1.05 V versus RHE, respectively. Although there appears to be some variations in the potential of these reactions, the key point is that they all always occur at more positive potentials than the hydrogen evolution potential (0 V versus RHE). Hence, bare Cu₂O can be easily degraded when in direct contact with the

aqueous solution, especially when illuminated to generate conduction band electrons under PEC conditions.

Figure 1b shows cyclic voltammetry (CV) curves of bare Cu₂O NW photocathodes in pH 5 electrolyte under dark and light conditions, after 5 CV scans. One reduction peak was observed at the potential of 0.4 V versus RHE under dark condition, while it was observed at the potential of 0.3 V versus RHE under one sun illumination. They are positioned in the potential range for reducing Cu₂O, indicating the transformation of Cu₂O into Cu. Interestingly, the current density at the reduction peak under one sun illumination (-4.52 mA cm⁻²) was larger than one under dark condition (-2.21 mA cm⁻²). It means that the transformation of Cu₂O into Cu is more active under illumination because a greater amount of photoexcited electrons can involve in the reduction reaction, indicating that the light induces more active Cu₂O degradation. On the other hand, two oxidation peaks were observed during the anodic sweep. The dominant oxidation peak under dark condition was at 0.75 V versus RHE. In comparison, under light condition, the peak at 0.6 V versus RHE was the dominant one. This indicates that the transformation into Cu(OH)₂ is more favorable under dark condition, whereas, the transformation into CuO is more favorable under light condition. Overall, the reduction and oxidation potentials of bare Cu₂O in aqueous electrolyte agreed with the literature, as presented in Figure 1a. These data provide us a “fingerprint” of the corrosion process of Cu₂O, which will be useful in diagnosing the full devices later in the study.

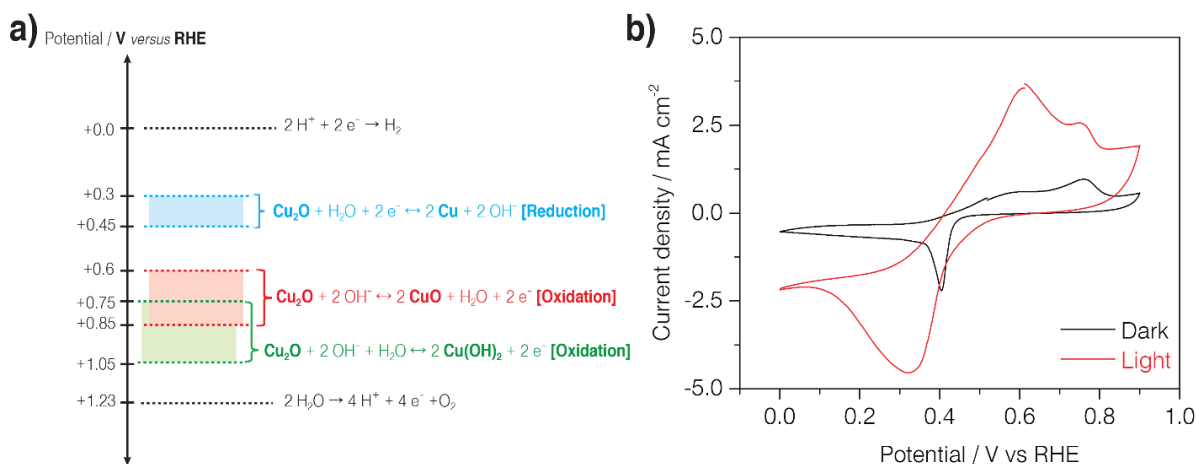


Figure 1. (a) Redox reaction potential windows of Cu₂O in terms of RHE scale. (b) CV curves of bare Cu₂O NW photocathodes in pH 5 electrolyte under dark (black) and light (red) conditions after 5 scans with a scan rate of 100 mV s⁻¹.

To check the compositional and morphological changes associated with these corrosion reactions, we carried out the chronoamperometry (CA) measurement of bare Cu₂O NW photocathodes in pH 5 electrolyte at applied potentials of HER (0 V versus RHE) and oxygen evolution reaction (OER, 1.23 V versus RHE) under dark condition for 100 min. As a result, the metallic Cu peaks (JCPDS 04-0836) were dominantly observed in the X-ray diffraction (XRD) pattern after the CA measurement at HER potential (Figure 2a), indicating that the Cu₂O was reduced to metallic Cu. In addition, the smooth NW structure changed into a rough structure with many grains, as shown in Figure 2b, which was due to the metallic Cu converted from the surface of Cu₂O NW. These metallic Cu grains were reformed or merged on the

surface of Cu_2O NW through the Cu_2O reduction reaction. On the other hand, $\text{Cu}(\text{OH})_2$ (JCPDS 13-0420) and $\text{Cu}(\text{OH})_2 \cdot \text{H}_2\text{O}$ (JCPDS 42-0638) phases appeared in the XRD pattern after the CA measurement at OER potential, as shown in Figure 2c. Furthermore, the NW structure was entirely transformed into the flake structure, as shown in Figure 2d. Based on these observations, it is estimated that the $\text{Cu}(\text{OH})_2$ flakes were covered on the Cu_2O NW structures because Cu_2O peaks were still dominant in the XRD pattern (Figure 2c). Thus, bare Cu_2O NW photocathodes would lose their original composition and morphology during the PEC water splitting process by the reduction and oxidation reactions. The most compositional and morphological degradation of bare Cu_2O NW photocathodes occurs in the initial stage of reactions (Figure S1). As a result, the bare Cu_2O NW photocathodes lose their initial PEC performances in few minutes during operation. Therefore, suitable protection strategies are demanded for durable PEC water splitting using Cu_2O NW photocathodes, even in the near neutral aqueous solution.

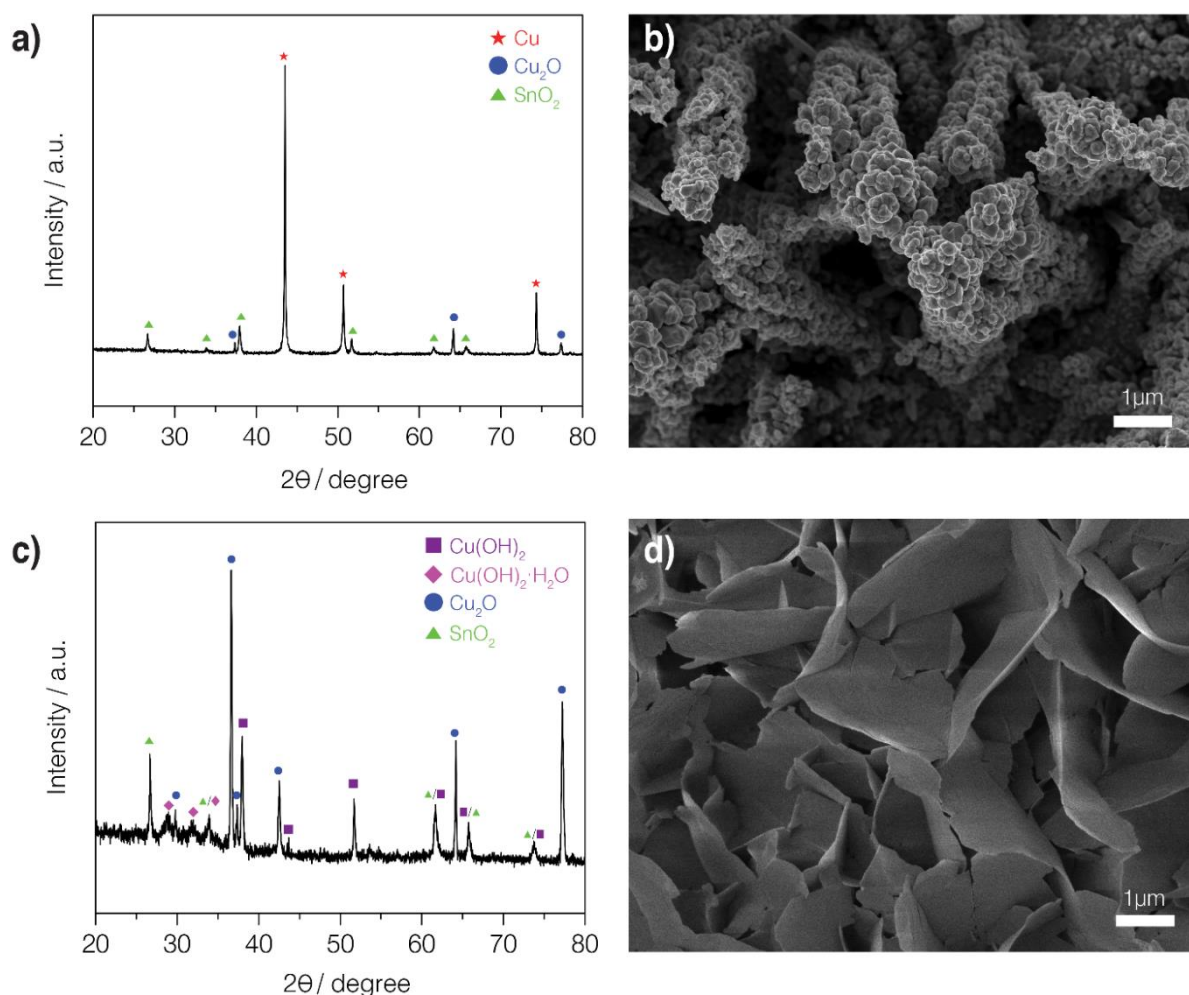


Figure 2. XRD patterns and SEM images of bare Cu_2O NW photocathodes after CA measurement in pH 5 electrolyte under dark condition for 100 min biased at (a,b) HER potential (0 V versus RHE) and (c,d) OER potential (1.23 V versus RHE). XRD peaks were indexed using following JCPDS files: Cu (JCPDS 04-0836), $\text{Cu}(\text{OH})_2$ (JCPDS 13-0420), $\text{Cu}(\text{OH})_2 \cdot \text{H}_2\text{O}$ (JCPDS 42-0638), Cu_2O (JCPDS 05-0667) and SnO_2 (JCPDS 41-1445).

Stability of Cu₂O NW Photocathodes with Overlayers and Catalysts: Platinum (Pt) versus RuO_x. It was demonstrated that atomic layer deposition (ALD) deposited amorphous TiO₂ thin films could prevent Cu₂O degradation in near-neutral conditions by acting as a corrosion protection layer to enable durable PEC performance.^{1,2} On the other hand, HER catalysts are directly exposed to the aqueous solution during the PEC operation because they are generally deposited on the surface of the TiO₂ protection layer.^{10,11} Therefore, it can also be a critical factor affecting the stability of Cu₂O photocathodes. Indeed, the evidence for this hypothesis was observed in previous research on the planar Cu₂O photocathodes.¹⁰ The PEC performance of Cu₂O/AZO/TiO₂ photocathodes with Pt catalysts decreased rapidly under continuous illumination. In contrast, those with RuO_x catalysts maintained high performance during long-term stability testing in the near-neutral aqueous solution. The PEC performance of Cu₂O/AZO/TiO₂ photocathodes with Pt catalysts could be recovered after re-depositing Pt catalysts, suggesting that physical loss of Pt during operation could explain the performance decreases.

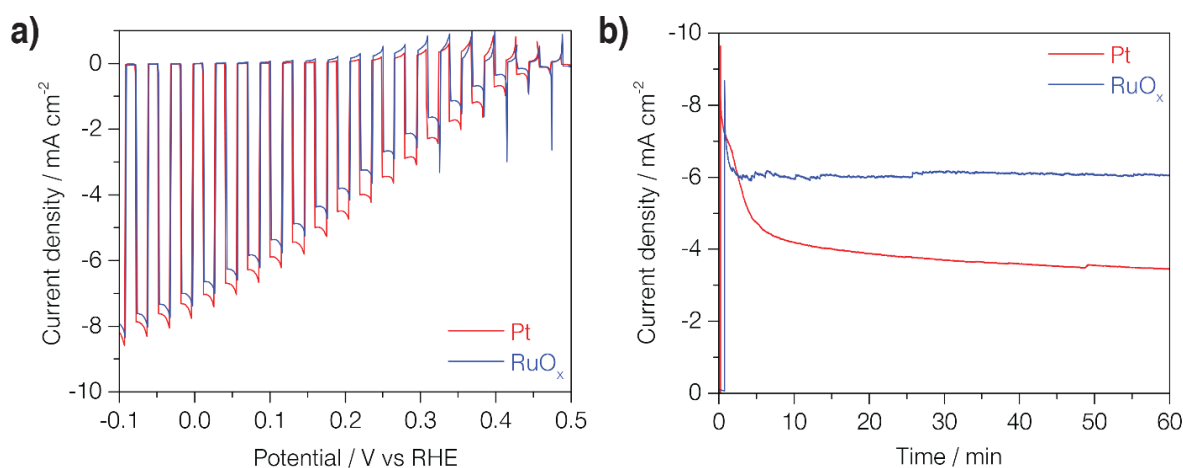


Figure 3. (a) J-E characteristics of samples under chopped one sun illumination and (b) current densities of samples during the CA stability measurement biased at 0V versus RHE under continuous illumination from LED lamp for 60 min. All measurements were carried out in pH 5 electrolyte. Cu₂O NW/AZO/TiO₂ photocathodes with Pt (red) and RuO_x (blue) catalysts were used as samples for measurement.

To verify this phenomenon and the hypothesis, AZO/TiO₂ coated Cu₂O NW (Cu₂O NW/AZO/TiO₂) photocathodes with Pt or RuO_x catalysts were compared in this study. Figure 3a shows the current density-potential (J-E) characteristics of Pt and RuO_x catalyzed Cu₂O NW/AZO/TiO₂ photocathodes in pH 5 electrolyte. The initial PEC performance including onset potential and current density was similar in both cases. However, they showed different PEC performances during the CA stability measurement biased at 0 V versus RHE for 60 min, as illustrated in Figure 3b. In the case of Pt catalyzed Cu₂O NW/AZO/TiO₂ photocathodes, the current density rapidly decreased within initial 10 min, followed by a gradually decrease later. In comparison, RuO_x catalyzed Cu₂O NW/AZO/TiO₂ photocathodes showed much more stable operation. These trends are in good agreement with planar Cu₂O photocathodes in the previous research.¹⁰

Figure 4 shows scanning electron microscope (SEM) and transmission electron microscope (TEM) images of Pt catalyzed Cu_2O NW/AZO/ TiO_2 photocathodes with element mapping of Pt before (Figure 4a-c) and after (Figure 4d-f) the CA stability measurement for 60 min. No huge differences and damages were observed in AZO/ TiO_2 coated Cu_2O NW structure after stability measurement. However, the surface status was significantly different. It was very smooth before measurement (Figure 4a), while many particles were observed on the surface after measurement (Figure 4d). Before stability measurement, Pt catalysts were homogeneously covered on the surface of Cu_2O NW/AZO/ TiO_2 photocathodes (Figure 4b,c), showing the smooth surface. In contrast, they were peeled off or aggregated into big nanoparticles after measurement (Figure 4e,f). The decrease in active Pt surface area likely causes the gradually decreased PEC performance for Pt catalyzed Cu_2O NW/AZO/ TiO_2 photocathodes during the stability measurement. This is a more direct evidence on the physical loss of Pt during PEC operation, as mentioned in previous research.¹⁰ In contrast, for RuO_x catalyzed Cu_2O NW/AZO/ TiO_2 photocathodes, no surface and structural changes were observed after stability measurement (Figure S2). This indirectly indicates that RuO_x catalysts on the Cu_2O NW/AZO/ TiO_2 photocathodes are robust during the PEC operation, which leads to the stable PEC performance of Cu_2O NW photocathodes. We attribute this to the different bond strength of Pt and RuO_x with TiO_2 . Ru-O bonds are dominantly formed in the RuO_x photodeposition,³² while Pt-O and Pt-Pt bonds are formed in the Pt photodeposition.³³ Based on the bond dissociation energies of each bond (Ru-O: 528 kJ/mol, Pt-O:418.6kJ/mol and Pt-Pt: 306.7 kJ/mol),³⁴ it could be estimated that the RuO_x catalyst is more robust with TiO_2 than the Pt catalyst. Based on these observations, the choice of HER catalysts is critical for the efficient and durable PEC performance of Cu_2O NW photocathodes, even when employing a TiO_2 protection layer and operating in near-neutral pH conditions.

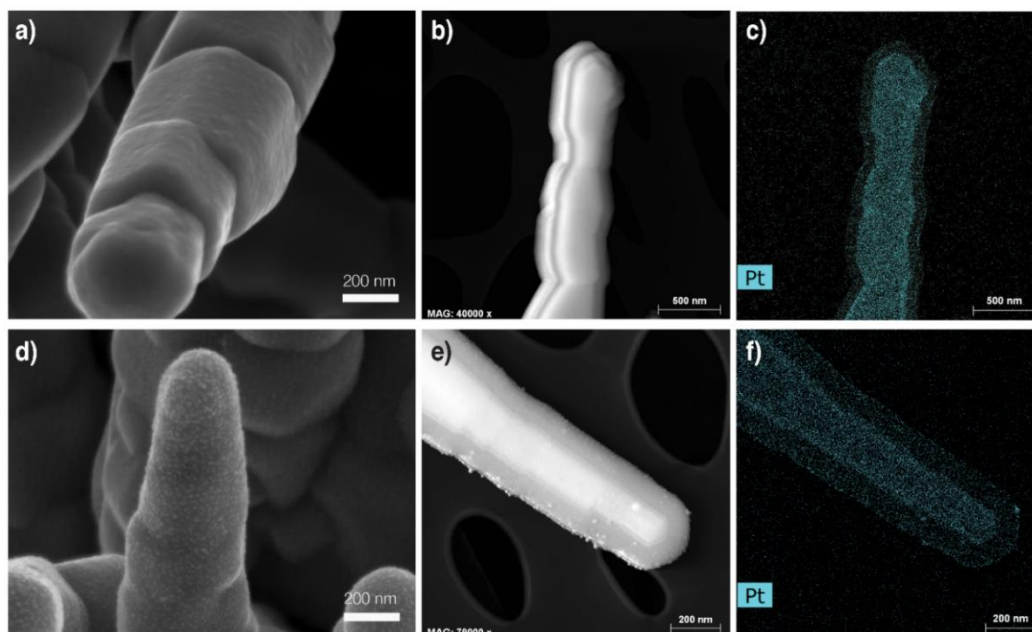


Figure 4. Morphologies of Pt catalyzed Cu_2O NW/AZO/ TiO_2 photocathodes (a-c) before and (d-f) after the CA stability measurement biased at 0V versus RHE in pH 5 electrolyte for 60 min: (a, d) SEM images and (b, c, e, f) TEM images and ones with element mapping of Pt.

Chemical and PEC Stability of Cu_2O NW/AZO/ TiO_2 / RuO_x Photocathodes. Cu_2O NW/AZO/ TiO_2 photocathodes with RuO_x HER catalysts (Cu_2O NW/AZO/ TiO_2 / RuO_x photocathodes) are generally stable for many hours (over 50 hr) in the near-neutral aqueous solution.¹² However, it is desirable to operate Cu_2O photocathodes in alkaline or acidic solutions to minimize pH gradients and cell resistance.^{26,27} To date, there are no reports on stable Cu_2O photocathodes in extreme acidic or alkaline solution irrespective of the existence of TiO_2 protection layer. In fact, the Pourbaix diagram for titanium predicts TiO_2 to be the stable phase under HER conditions across a wide range of pH values, except for extreme acid. However, our previous experiments revealed these Cu_2O /AZO/ TiO_2 devices to be generally unstable when operated in acidic or alkaline solutions, which suggests that the degradation is dependent on the pH condition.²⁸ The degradation mechanism of Cu_2O photocathodes in these harsh conditions remains unclear. Therefore, we investigated the chemical and PEC stability of Cu_2O NW/AZO/ TiO_2 / RuO_x photocathodes in strong acidic and alkaline solutions.

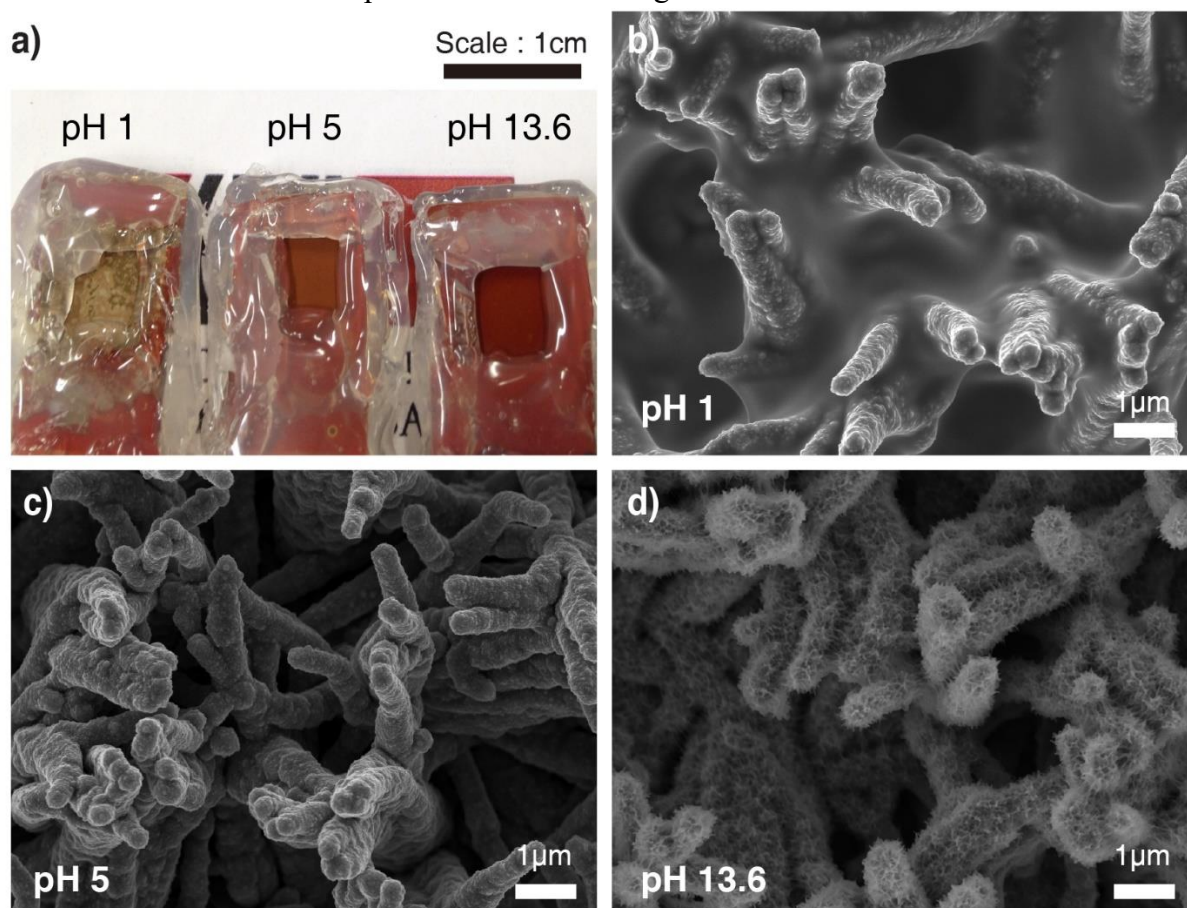


Figure 5. (a) Cu_2O NW/AZO/ TiO_2 / RuO_x photocathodes after soaking test in different pH electrolytes: 0.1M H_2SO_4 (pH 1), 0.1 M $\text{KH}_2\text{PO}_4/0.5$ M Na_2SO_4 (pH 5) and 1M KOH (pH 13.6). SEM images of Cu_2O NW/AZO/ TiO_2 / RuO_x photocathodes after soaking test in (b) pH 1, (c) pH 5 and (d) pH 13.6 electrolyte, respectively. The soaking test was carried out under dark condition for 20 hr.

To observe chemical stability of Cu_2O NW/AZO/ TiO_2 / RuO_x photocathodes, the Cu_2O NW/AZO/ TiO_2 / RuO_x photocathodes were soaked in the dark for 20 hr in aqueous solutions of

different pH as follows: 0.1M H₂SO₄ (pH 1), 0.1 M KH₂PO₄/0.5 M Na₂SO₄ (pH 5) and 1M KOH (pH 13.6). Figure 5a shows Cu₂O NW/AZO/TiO₂/RuO_x photocathodes after soaking test for 20 hr in the three different electrolytes under dark condition. The severe damage of Cu₂O NW photocathodes could be observed by the naked eye in pH 1 electrolyte. The strong acidic condition led to the etching or dissolution of components in Cu₂O NW photocathodes, as observed in Figure 5b. On the other hand, no obvious physical damages were observed by visual inspection after soaking test for 20 hr in pH 5 and pH 13.6 electrolytes.

Interestingly, the morphological differences were also observed in these two samples by SEM and TEM images with elemental mapping. As shown in Figure 5c, the morphology of the Cu₂O NW/AZO/TiO₂/RuO_x photocathode remained unchanged after soaking test in pH 5 electrolyte for 20 hr, compared to the one before soaking test (Figure S3). Furthermore, it was demonstrated that all components including Cu₂O NW, AZO/TiO₂ overlayers and RuO_x catalysts were well-preserved after soaking test (Figure S4). This provides the physical evidence for the endurance of Cu₂O NW/AZO/TiO₂/RuO_x photocathodes in pH 5 electrolyte. On the other hand, the smooth surface of the NWs transformed into wrinkled structures with spikes (Figure 5d) after soaking test in pH 13.6 electrolyte. The wrinkled structures were confirmed in the HAADF TEM image, as shown in Figure 6a. According to the TEM images with detailed elemental mappings (Figure 6b-f), the core of Cu₂O NW, AZO overlayer and RuO_x catalysts showed no obvious changes, while the amorphous TiO₂ overlayer transformed into a wrinkled structure and some Cu was detected on the surface of the wrinkled TiO₂ structure.

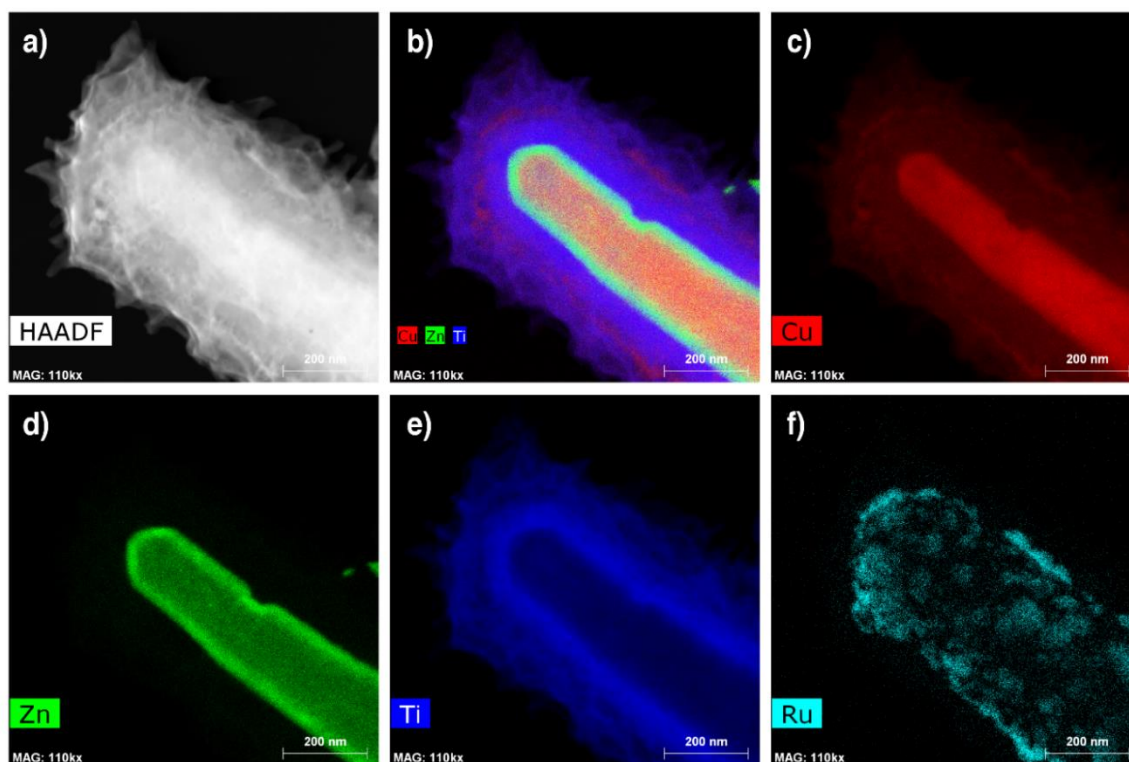
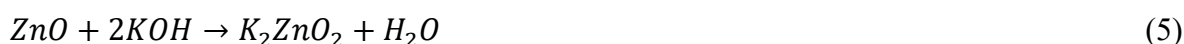


Figure 6. TEM and energy-dispersive X-ray (EDX) characterization of Cu₂O NW/AZO/TiO₂/RuO_x photocathodes after soaking test in pH 13.6 electrolyte for 20 hr: (a) HAADF image and element mapping images of (b) combination, (c) Cu, (d) Zn, (e) Ti and (f) Ru, respectively.

In strong alkaline solution, the TiO_2 thin film can be dissolved through the following reaction.^{35,36}



Then, the TiO_2 layer can be rearranged by reacting HTiO_3^- products with TiO_2 and H_2O .³⁷ As a result, the TiO_2 thin film was expanded to the wrinkled layer after soaking test for 20 hrs in pH 13.6 electrolyte (Figure 6e). This layer fully covered the RuO_x catalysts (Figure 6f). On the other hand, since the AZO layer is based on ZnO , it can react with the alkaline solution based on KOH through the following reaction.³⁸



The H_2O from this reaction attacks the Cu_2O NW core. Subsequently, Cu elements leached out to the surface (Figure 6c), while there are no changes of Zn elements (Figure 6d). These could be critical factors to reduce the PEC performance of Cu_2O NW photocathodes in strong alkaline aqueous solutions during dark periods (e.g. nighttime) between PEC operation.

It was demonstrated that light could accelerate the degradation of bare Cu_2O NW photocathodes in the first section. In the following, the PEC degradation of Cu_2O NW/AZO/ TiO_2 / RuO_x photocathodes in aqueous solutions with different pH conditions was explored. For this, we measured the PEC performance of Cu_2O NW/AZO/ TiO_2 / RuO_x photocathodes in each electrolyte using linear sweep voltammetry (LSV) with several scans under simulated one sun illumination. In pH 5 electrolyte, no degraded PEC performances were observed even after several LSV scans (Figure S5a). On the contrary, the PEC performances were gradually enhanced along with continuous LSV scans due to the RuO_x catalyst activation.¹⁰ After several LSV scans, it became stable and showed negligible dark currents (Figure S5b). It confirms that Cu_2O NW photocathodes with the TiO_2 protection layer is quite stable in the near-neutral aqueous solution during PEC water splitting, which is in good agreement with the results in the previous section and previous results.¹²

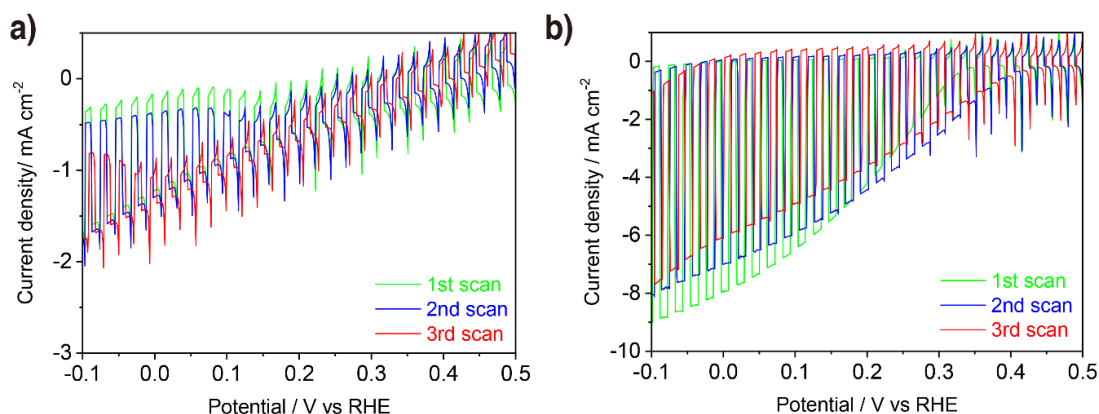


Figure 7. J-E characteristics of samples under chopped one sun illumination using LSV measurements in (a) pH 1 and (b) pH 13.6 electrolytes. AZO/ TiO_2 overlayers Cu_2O NW photocathodes with RuO_x catalysts were used as samples for measurement.

On the other hand, the $\text{Cu}_2\text{O NW/AZO/TiO}_2/\text{RuO}_x$ photocathodes instantly showed abnormal behaviors of the PEC performance in the electrolytes with strong acidic and alkaline conditions. In pH 1 electrolyte, the sample showed poor PEC performances even in the first LSV scan (Figure 7a). Furthermore, its dark current increased in accordance with continuous LSV scans. It was likely due to the severe visual damage with many white spots were observed in the sample (Figure S6b). It includes two morphological changes, detected by SEM images: one is the NW structures with many grains (Figure 8a) and the other is the collapsed NW structures (Figure 8b). The former is similar to the structure with the coverage of metallic Cu on the surface in Figure 2b, while the latter is similar to the structure in Figure 5b. The etching or dissolution of AZO/ TiO_2 overlayers and RuO_x catalyst facilitates the core of $\text{Cu}_2\text{O NW}$ to expose to the electrolyte, resulting in the transformation of Cu_2O into metallic Cu. Therefore, we can conclude that morphological and compositional changes of $\text{Cu}_2\text{O NW}$ due to the attack of strong acidic electrolyte are main degradation factors for $\text{Cu}_2\text{O NW/AZO/TiO}_2/\text{RuO}_x$ photocathodes during PEC operation in strong acidic condition.

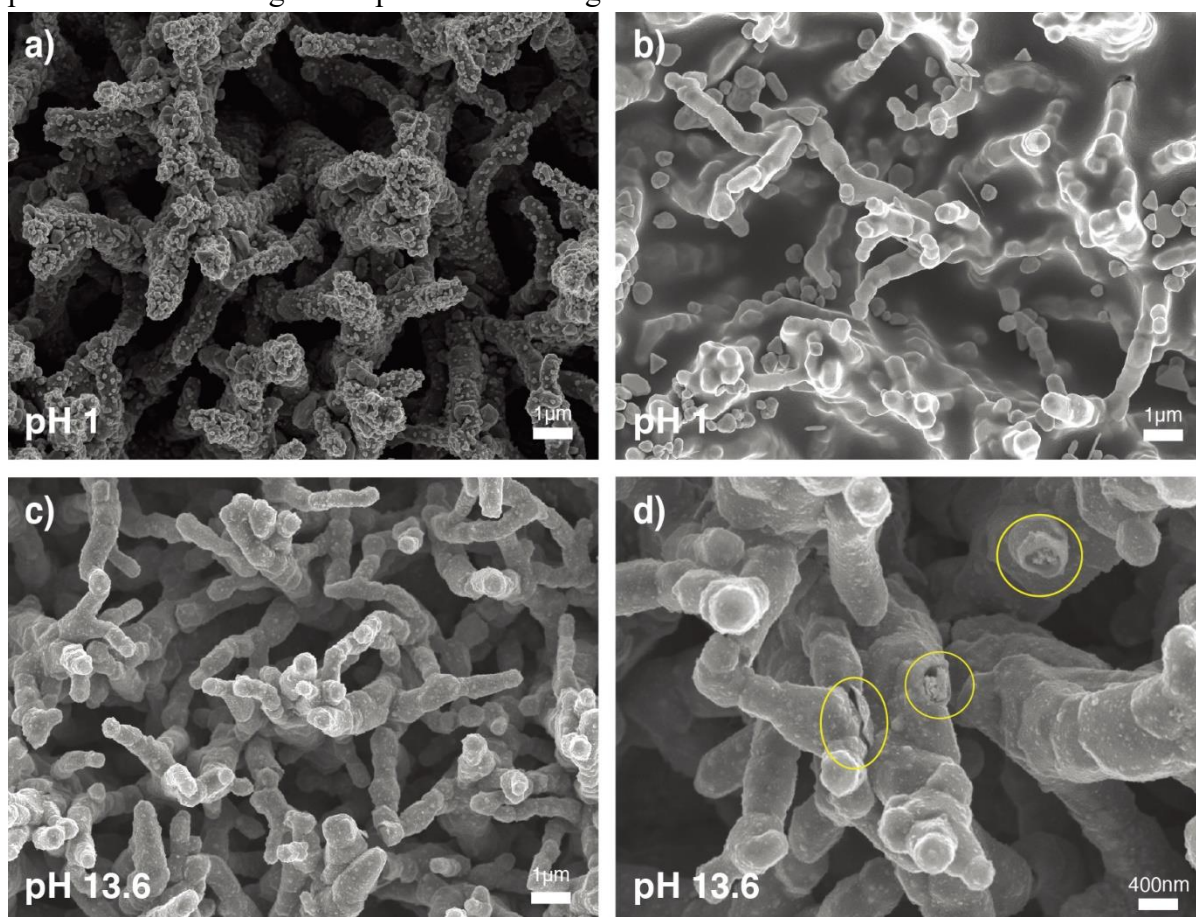


Figure 8. SEM images of $\text{Cu}_2\text{O NW/AZO/TiO}_2/\text{RuO}_x$ photocathodes after three scans of LSV measurement under illumination: (a, b) Different parts of samples tested in pH 1 electrolyte, (c) Samples tested in pH 13.6 electrolyte at low magnification and (d) high magnification. Cracked and hollow structures are observed in the yellow circles.

In comparison, in pH 13.6 electrolyte, the $\text{Cu}_2\text{O NW}$ photocathodes showed the decent PEC

performances with less dark current in terms of current density in the first LSV scan (Figure 7b). It indicates that the degradation in the strong alkaline condition is a little bit slower than one in the strong acidic condition. However, the current density gradually degraded from the second LSV scan onwards along with the increased dark current at the negative potential. Counter-intuitively, significant morphological damages were not observed by SEM imaging at low magnification (Figure 8c). Looking into detail, the cracked and hollow structures can be partially observed in the SEM image at high magnification (Yellow circles in Figure 8d). These could be formed through defects on the TiO₂ protection layer. These cracks exposed the Cu₂O below the TiO₂ overlayer to the electrolyte. Hence, the Cu₂O was transformed into Cu(OH)₂ under PEC test, coinciding with formation of sections with the blueish color on the sample surface (Figure S6c). Consequently, the Cu₂O NW photocathodes lost their PEC performances in the strong alkaline electrolyte under PEC operation.

In summary, the degradations of Cu₂O NW/AZO/TiO₂/RuO_x photocathodes in extreme acidic or alkaline electrolytes are morphological and compositional, which seem to result from instability of the amorphous TiO₂ ALD films under these conditions. In terms of the morphology, the whole Cu₂O NW structures were damaged in the strong acid electrolyte, while the morphology of TiO₂ overlayer was changed in the strong alkaline electrolyte. Regarding the composition, Cu₂O transformed into metallic Cu in the strong acid solution, while it partially changed into Cu(OH)₂ in the strong alkaline solution. The Pourbaix diagram of Cu also supports these compositional degradations.²⁸ These are mainly caused by the instability of the amorphous TiO₂ protection layer in the strong acid and alkaline solutions. Interestingly, in alkaline electrolyte, the degradation of Cu₂O NW photocathodes was totally different when the sample was soaked in dark (Figure 5d) and measured under illuminated PEC conditions (Figure 8d). The slow transformation of amorphous TiO₂ protection layer was occurred by the strong alkaline solution in the dark, while the PEC performance rapidly decreased due to the defects on the TiO₂ protection layer under illumination. This suggests there are different degradation mechanism of Cu₂O NW photocathodes, which depend on the operating condition (i.e. potential), and are important to consider given the need for future PEC devices to survive through repeated day-night cycles. Overall, the results indicate that the present protection strategy using amorphous TiO₂ ALD layers on Cu₂O NW photocathodes is not yet adequate for durable PEC water splitting in aqueous solutions with extreme pH conditions. Therefore, more robust protection layers with less defects are demanded for achieving stable Cu₂O NW photocathodes.

Feasibility of the Crystalline TiO₂ Protection Layer for Better Stability. Crystalline TiO₂ is considered as a more effective protection layer for PEC electrodes compared to amorphous TiO₂, because it is less permeable to protons and hydroxyl ions and more resistant to electron traps.³⁹ In general, annealing process at high temperature above 350 °C is necessary to get crystalline TiO₂.⁴⁰ However, it is challenging for Cu₂O photocathodes because Cu₂O is quite sensitive to such high temperature. Hence, Cu₂O photocathodes with heat treatment to apply the crystalline TiO₂ protection layer always show decreased PEC performance. It has been discussed in the literature that it is caused by loss of doping or catalytic characteristics of Cu₂O in the fabrication process.^{21,41} Nevertheless, the exact reason for this is still unclear.

To investigate this, the properties of Cu_2O NW/AZO/ TiO_2 photocathodes following heat treatment in Ar at different temperatures were characterized. Figure 9a shows XRD patterns of Cu_2O NW/AZO/ TiO_2 photocathodes after annealing under Ar flow at different temperatures of 250 °C, 350 °C and 450 °C, respectively. The cubic Cu_2O peaks (JCPDS 05-0667) were clearly observed in all XRD patterns, and no additional peaks due to different possible Cu-O phase emerged. This indicates that there was no noticeable oxidation or reduction of Cu_2O in the heat treatment process under Ar flow. No crystalline TiO_2 peaks were observed for samples without annealing or after annealing at 250 °C, indicating that the TiO_2 protection layer was still amorphous. For samples annealed at or above 350 °C, XRD peaks attributable to (101) and (200) planes of anatase TiO_2 (JCPDS 21-1272) were observed at $2\theta = 25.2^\circ$ and 48.0° , respectively. This suggests some crystallization of the amorphous TiO_2 protection layer occurs with a transition somewhere between 250-350 °C. Thus, it is demonstrated that the heat treatment under Ar flow at temperature above 350 °C induced some crystallization of TiO_2 without noticeably changing the crystalline composition of Cu_2O .

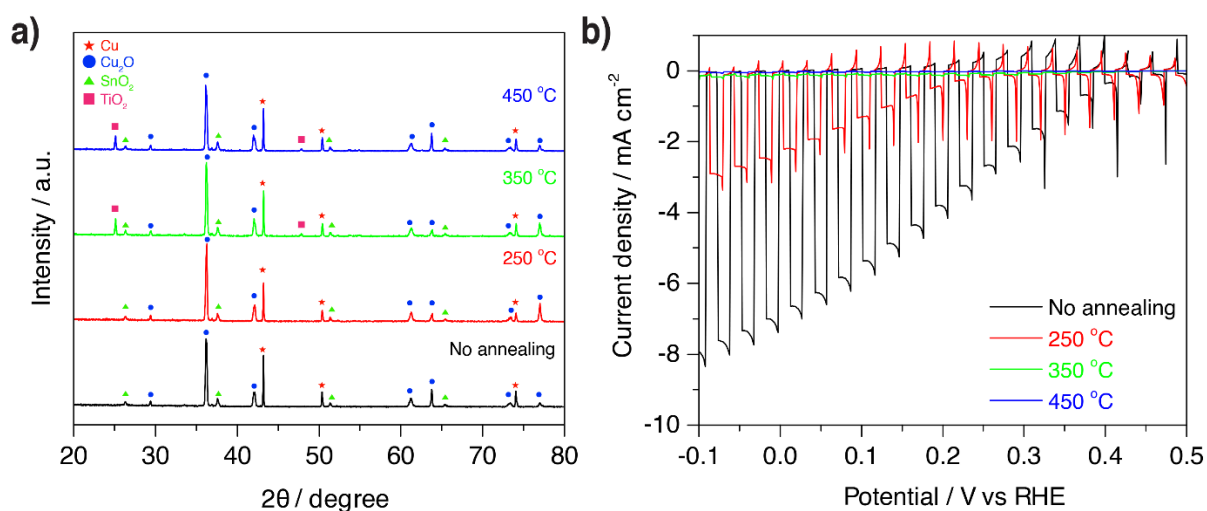


Figure 9. (a) XRD patterns of Cu_2O NW/AZO/ TiO_2 photocathodes before (black, no annealing) and after annealing under Ar flow for 1 h at different temperatures: 250 °C (red), 350 °C (green) and 450 °C (blue). XRD peaks were indexed using following JCPDS files: Cu (JCPDS 04-0836), Cu_2O (JCPDS 05-0667), SnO_2 (JCPDS 41-1445) and TiO_2 (JCPDS 21-1272). (b) J-E characteristics of each sample with RuO_x catalyst under chopped one sun illumination in pH 5 electrolyte.

Figure 9b shows the J-E characteristics of RuO_x catalyzed Cu_2O NW/AZO/ TiO_2 photocathodes with the heat treatment at different temperatures under chopped one sun illumination in pH 5 electrolyte. The PEC performance in terms of photocurrent and onset potential was decreased, whereas the dark current remained low for all samples, suggesting that TiO_2 protection layer retained its ability to prevent Cu_2O corrosion after annealing. Following each of the annealing treatments, the protection layer seemingly remained intact, the Cu_2O appeared stable in composition (based on the XRD above), and no significant structural changes were apparent by SEM analysis (Figure 10a, Figure S7). Thus, the exact reason for the decreased PEC performance by the heat treatment is revealed in detail by the TEM structural analysis with elemental mapping in the next paragraph. On the other hand, the photoresponse

was almost negligible for samples annealed above 350 °C, which is a temperature starting the crystallization of TiO₂ protection layer. Hence, the further PEC measurement was not carried out in either acid or alkaline solution. In addition, it was unfortunately difficult to study the effect of crystalline TiO₂ protection layer on the stability of Cu₂O photocathodes because the J-E performances were negligible.

TEM images with elemental mapping of Cu₂O NW/AZO/TiO₂ photocathodes after annealing at 450 °C are shown in Figure 10 b-f. Although there were no noticeable changes to the NW array or individual NW surface structures (Figure 10a), significant changes were observed inside the NWs. While the AZO/TiO₂ overlayers appeared well-preserved (Figure 10e-f), the Cu₂O NWs became fragmented (Figure 10d) which appears to result from a volume contraction or recrystallization due to the heat treatment. The resulting greatly diminished PEC performance was likely due to the loss in electronic continuity of the Cu₂O NWs along which holes cannot diffuse to be collected by the external circuit. This observation is somewhat puzzling, since the initial Cu₂O NW array synthesis method employs heating in Ar at an even higher temperature (600 °C) and for a longer duration, conditions which yield continuous and crystalline phase-pure Cu₂O NWs. It seems the presence of the overlayers plays a role in inducing this heat-induced segregation of Cu₂O domains, perhaps by stabilizing individual crystalline grains and helping them recrystallize into discontinuous particles. It is likely due to the different thermal expansion coefficients between the Cu₂O core and AZO/TiO₂ shell. Whether this effect coincides directly with the formation of crystalline TiO₂ remains unclear, and will be a subject of follow-up study. Furthermore, besides these observed structural changes, it is known that p-n heterojunction interfaces can be sensitive to temperature, wherein diffusion of ions or dopants can significantly affect the interfacial electronic structure^{2,42}.

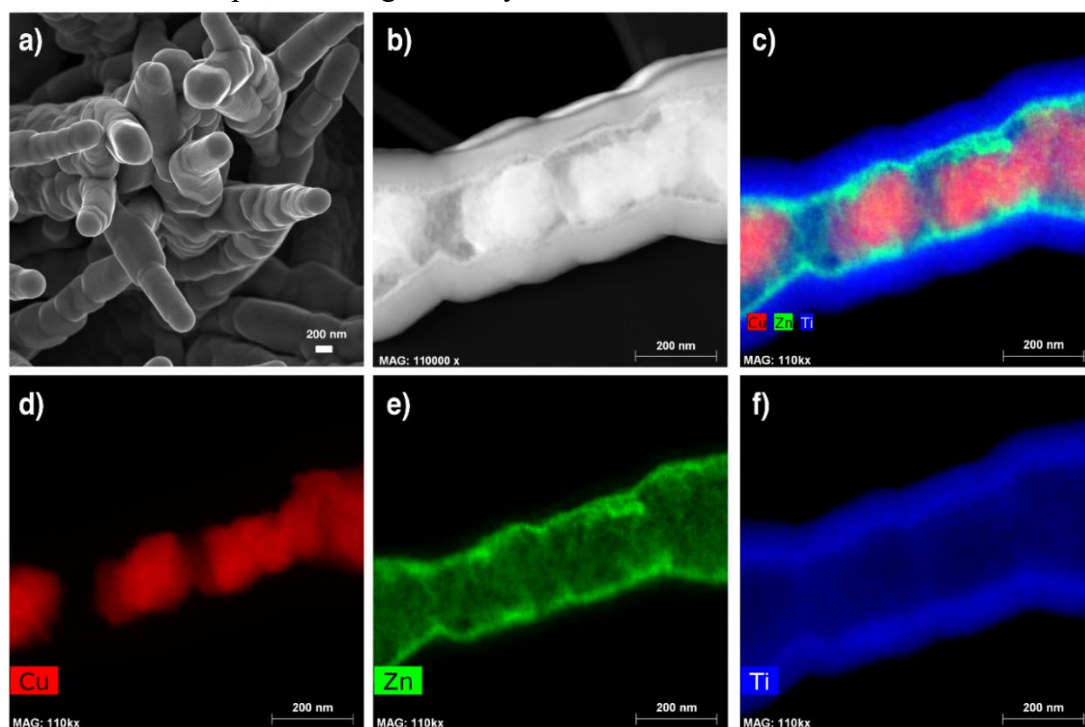


Figure 10. Morphological characterization of Cu₂O NW/AZO/TiO₂ photocathodes after annealing at 450 °C under Ar flow for 1 hr: (a) SEM image, (b) HAADF TEM image and element mapping images of (c) combination, (d) Cu, (e) Zn and (f) Ti, respectively.

Based on these observations, direct heat treatment is not a suitable method to crystallize the TiO₂ protection layer for improving the stability of Cu₂O NW photocathodes, as well as the PEC performance. Therefore, alternative methods to deposit crystalline TiO₂ protection layer on Cu₂O NW photocathodes without damaging Cu₂O, as well as exploration of alternative protection materials, should be pursued for achieving efficient and durable Cu₂O NW photocathodes.

CONCLUSIONS

Since bare Cu₂O NW are unstable for aqueous PEC water splitting, protection layers are essential for making durable Cu₂O-based photocathodes. Indeed, the amorphous TiO₂ overlayer plays an important role in preventing the degradation of Cu₂O NW photocathodes in the electrolytes with mild pH conditions. However, it does not work effectively in the electrolytes with extreme pH conditions because it will be etched away by the strong acidic solution or transformed in the strong alkaline solution, which leads to morphological changes and corrosion of Cu₂O NW photocathodes.

Thus, to achieve efficient and durable PEC water splitting with Cu₂O NW photocathodes, improvements to amorphous TiO₂ should be developed. Crystalline TiO₂ could be a feasible route to improvement, but crystallization of amorphous TiO₂ generally requires high temperatures above 350 °C, which is detrimental to the Cu₂O as it leads to the restructuring of Cu₂O, resulting in disconnected NW structures. In summary, alternative protection layers should meet the criteria as follows: (1) resistance to the strong acidic or alkaline aqueous solutions; (2) pinhole-free structure; (3) its fabrication process should not cause structural and compositional changes of Cu₂O NW photocathodes, as well as other optoelectronic properties.⁴³ In addition, the strong binding with HER catalysts should also be considered because the detachment of catalysts from the protection layer can lead to decreased PEC performances. Investigations on the dual-functional overlayer including HER catalytic activity and protection function are also a promising approach for achieving efficient and durable Cu₂O NW photocathodes.

EXPERIMENTAL SECTION

Preparation of Cu₂O NW Photocathodes. Cu₂O NW photocathodes were fabricated by the same procedure as described in our previous work.¹² Briefly, Cu was deposited on cleaned fluorine doped tin oxide coated glass (FTO, TEC-15, G2E) substrates by DC sputtering (DP-650, Alliance-Concept) at room temperature to a Cu thickness of 1.5 μm. The Cu layer was subsequently anodized in 3 M KOH solution to form Cu(OH)₂ NW. The anodized samples were transformed into Cu₂O NW by annealing at 600 °C for 4 hr under Ar flow. Bare Cu₂O NW photocathodes were completed by further electrodepositing a Cu₂O thin layer as blocking layer in a lactate-stabilized copper sulfate solution (pH 12) applying a current density of -0.1 mA cm⁻² for 30 min. A 20 nm thick AZO and a 100 nm thick TiO₂ were deposited by ALD (Savannah 100, Cambridge Nanotech) for making a p-n junction and a protection layer, respectively. For HER catalyst depositions, Cu₂O NW/AZO/TiO₂ photocathodes were functionalized by either RuO_x or Pt by photoelectrochemical deposition for 400 sec under one

sun illumination. RuO_x deposition was carried out in 1.3 mM potassium perruthenate (KRuO₄) solution with a current density of -28.3 μA cm⁻², while Pt deposition was implemented in 1 mM chloroplatinic acid (H₂PtCl₆) solution with a current density of -8.5 μA cm⁻² as described previously.¹⁰ For making a crystalline TiO₂ protection layer on the Cu₂O NW photocathodes, Cu₂O NW/AZO/TiO₂ photocathodes were annealed at different temperatures for 1 hr with 5 °C min⁻¹ ramping under Ar flow in a tube furnace before catalyst deposition. The annealed samples were naturally cooled down to the room temperature.

Electrochemical Characterization and Stability Test. All electrochemical characterization measurements were carried out using a three-electrode configuration, consisting of the working electrode, the counter electrode (typically Pt wire) and the reference electrode of Ag/AgCl in saturated KCl. Electrolyte solution with near-neutral pH was 0.1 M KH₂PO₄ and 0.5 M Na₂SO₄ (pH 5). The electrolyte solution with extreme pH conditions were 0.1 M H₂SO₄ (pH 1) as a strong acidic electrolyte and 1 M KOH (pH 13.6) as a strong alkaline solution, respectively. The PEC performance of Cu₂O NW photocathodes was measured by a potentiostat (SP 200, BioLogic Science Instruments) under chopped light illumination from a 100 W ozone free Xenon lamp equipped with an air mass (AM) 1.5G filter (Oriel LCS-100, Newport) calibrated to one sun illumination (100 mW cm⁻²). Scan rate was fixed as 10 mV s⁻¹ and its direction was from positive potential to negative potential during the PEC measurement. For the direct comparison of PEC performances according to different pH electrolytes, the measured potential was converted to the RHE scale using the equation: $V_{\text{RHE}} = V_{\text{Ag/AgCl}} + 0.197 \text{ V} + 0.059 \text{ V} \cdot \text{pH}$.

CV of bare Cu₂O NW photocathodes was measured in pH 5 electrolyte under dark and illuminated conditions to find out its redox potential. The potential was scanned between 0 V and 0.9 V versus RHE with a scan rate of 100 mV s⁻¹. For the chemical stability characteristics in different pH solutions, Cu₂O NW/AZO/TiO₂ photocathodes with RuO_x catalysts were soaked in different electrolytes without any external bias in the dark condition for 20 hours. In further experiments, CA was carried out at fixed potential of 0 V versus RHE, which is identical to the hydrogen evolution potential, to investigate the PEC stability characteristics. It was measured under the continuous light illumination from a “cold white” LED (ThorLabs) to minimize the heat influence on the degradation of Cu₂O NW photocathodes. It was calibrated to induce the same current density as Cu₂O NW photocathodes under one sun illumination.

Material Characterizations. The XRD patterns were acquired by a Bruker D8 Discover diffractometer equipped with a linear silicon strip “Lynx Eye” detector in Bragg-Brentano mode using Cu Kα radiation (1.540598 Å) and a Niβ-filter. Spectra were obtained from 2θ = 20° to 80° at a scan rate of 1° min⁻¹ with a step width of 0.02° and a source slit width of 1 mm. The morphology and structure of Cu₂O NW photocathodes were analyzed by a high-resolution SEM (ZEISS Merlin) and a high-resolution TEM (Technai Osiris, FEI). The composition of Cu₂O NW photocathodes was characterized by the EDX spectra obtained in STEM mode with Technai Osiris.

ACKNOWLEDGMENTS

This research was supported by the “Basic Science Research Program” funded by the Korea Institute of Ceramic Engineering and Technology, Republic of Korea (No. KPB21004). This work was supported by Ceramic Strategic Research Program (No. KPP20004-1) through Korea Institute of Ceramic Engineering & Technology. This research was supported by the program of Future Hydrogen Original Technology Development (NRF-2021M3I3A1084649), through the National Research Foundation of Korea (NRF), funded by the Korean government (Ministry of Science and ICT(MSIT)). This study was supported by the National Key Research and Development Program of China (Grant No. 2018YFB1502003; 2019YFE0123400), the National Natural Science Foundation of China (Grant No. 52072187), and the Strategic Japanese-Swiss Science and Technology Programme from the Swiss National Science Foundation (grant No. 514259).

REFERENCES

- (1) Paracchino, A.; Laporte, V.; Sivula, K.; Grätzel, M.; Thimsen, E. Highly Active Oxide Photocathode for Photoelectrochemical Water Reduction. *Nat. Mater.* **2011**, *10*, 456-461.
- (2) Paracchino, A.; Mathews, N.; Hisatomi, T.; Stefik, M.; Tilley, S.D.; Grätzel, M. Ultrathin Films on Copper(I) Oxide Water Splitting Photocathodes: A Study on Performance and Stability. *Energy Environ. Sci.* **2012**, *5*, 8673-8681.
- (3) Paracchino, A.; Brauer, J.C.; Moser, J.-E.; Thimsen, E.; Grätzel, M. Synthesis and Characterization of High-photoactivity Electrodeposited Cu₂O Solar Absorber by Photoelectrochemistry and Ultrafast Spectroscopy. *J. Phys. Chem. C* **2012**, *116*, 7341-7350.
- (4) Meyer, B.K.; Polity, A.; Reppin, D.; Becker, M.; Hering, P.; Klar, P.J.; Sander, T.; Reindl, C.; Benz, J.; Eickhoff, M.; Heiliger, C.; Heinemann, M.; Bläsing, J.; Krost, A.; Shokovets, S.; Müller, C.; Ronning, C. Binary Copper Oxide Semiconductors: From Materials towards Devices. *Phys. Status Solidi B* **2012**, *249*, 1487-1509.
- (5) Wick, R.; Tilley, S.D. Photovoltaic and Photoelectrochemical Solar Energy Conversion with Cu₂O. *J. Phys. Chem. C* **2015**, *119*, 26243-26257.
- (6) Dai, P.; Li, W.; Xie, J.; He, Y.; Thorne, J.; McMahon, G.; Zhan, J.; Wang, D. Forming Buried Junctions to Enhance the Photovoltage Generated by Cuprous Oxide in Aqueous Solutions. *Angew. Chem.* **2014**, *53*, 13493-13497.
- (7) Li, C.; Hisatomi, T.; Watanabe, O.; Nakabayahi, M.; Shibata, N.; Domen, K.; Delaunay, J.-J. Positive Onset Potential and Stability of Cu₂O-based Photocathodes in Water Splitting by Atomic Layer Deposition of a Ga₂O₃ Buffer Layer. *Energy Environ. Sci.* **2015**, *8*, 1493-1500.
- (8) Li, C.; Hisatomi, T.; Watanabe, O.; Nakabayahi, M.; Shibata, N.; Domen, K.; Delaunay, J.-J. Simultaneous Enhancement of Photovoltage and Charge Transfer in Cu₂O-based Photocathode Using Buffer and Protective Layers. *Appl. Phys. Lett.* **2016**, *109*, 033902.
- (9) Son, M.-K.; Steier, L.; Schreier, M.; Mayer, M.T.; Luo, J.; Grätzel, M. A Copper-nickel Mixed Oxide Hole Selective Layer for Au-free Transparent Cuprous Oxide Photocathodes. *Energy Environ. Sci.* **2017**, *10*, 912-918.
- (10) Tilley, S.D.; Schreier, M.; Azevedo, J.; Stefik, M.; Grätzel, M. Ruthenium Oxide Hydrogen Evolution Catalysis on Composite Cuprous Oxide Water-Splitting Photocathodes. *Adv. Funct. Mater.* **2014**, *24*, 303-311.

- (11) Morales-Guio, C.G.; Tilley, S.D.; Vrubel, H.; Grätzel, M.; Hu, X. Hydrogen Evolution from a Copper(I) Oxide Photocathode Coated with an Amorphous Molybdenum Sulphide Catalyst. *Nat. Commun.* **2014**, *5*, 3059.
- (12) Luo, J.; Steier, L.; Son, M.-K.; Schreier, M.; Mayer, M.T.; Grätzel, M. Cu₂O Nanowire Photocathodes for Efficient and Durable Solar Water Splitting. *Nano Lett.* **2016**, *16*, 1848-1857.
- (13) Pan, L.; Kim, J.H.; Mayer, M.T.; Son, M.-K.; Ummadisingu, A.; Lee, J.S.; Hagfeldt, A.; Luo, J.; Grätzel, M. Boosting the Performance of Cu₂O Photocathodes for Unassisted Solar Water Splitting Devices. *Nat. Catal.* **2018**, *1*, 412-420.
- (14) Schreier, M.; Gao, P.; Mayer, M.T.; Luo, J.; Moehl, T.; Nazeeruddin, M.K.; Tilley, S.D.; Grätzel, M. Efficient and Selective Carbon Dioxide Reduction on Low Cost Protected Cu₂O Photocathodes Using a Molecular Catalyst. *Energy Environ. Sci.* **2015**, *8*, 855-861.
- (15) Schreier, M.; Luo, J.; Gao, P.; Moehl, T.; Mayer, M.T.; Grätzel, M. Covalent Immobilization of a Molecular Catalyst on Cu₂O Photocathode for CO₂ Reduction. *J. Am. Chem. Soc.* **2016**, *138*, 1938-1946.
- (16) Chen, S.; Wang, L.-W. Thermodynamic Oxidation and Reduction Potentials of Photocatalytic Semiconductors in Aqueous Solution. *Chem. Mater.* **2012**, *24*, 3659-3666.
- (17) Wu, L.; Tsui, L.; Swami, N.; Zangari, G. Photoelectrochemical Stability of Electrodeposited Cu₂O Films. *J. Phys. Chem. C* **2010**, *114*, 11551-11556.
- (18) Amano, F.; Ebnia, T.; Ohtani, B. Enhancement of Photocathodic Stability of P-type Copper(I) Oxide Electrodes by Surface Etching Treatment. *Thin Solid Films* **2014**, *550*, 340-346.
- (19) Yang, Y.; Han, J.; Ning, X.; Su, J.; Shi, J.; Cao, W.; Xu, W. Photoelectrochemical Stability Improvement of Cuprous Oxide (Cu₂O) Thin Films in Aqueous Solution. *Int. J. Energy Res.* **2016**, *40*, 112-123.
- (20) Azevedo, J.; Tilley, S.D.; Schreier, M.; Stefik, M.; Sousa, C.; Araújo, J.P.; Mendes, A.; Grätzel, M.; Mayer, M.T. Tin Oxide as Stable Protective Layer for Composite Cuprous Oxide Water-Splitting Photocathodes. *Nano Energy* **2016**, *24*, 10-16.
- (21) Azevedo, J.; Steier, L.; Dias, P.; Stefik, M.; Sousa, C.T.; Araújo, J.P.; Mendes, A.; Grätzel, M.; Tilley, S.D. On the Stability Enhancement of Cuprous Oxide Water Splitting Photocathodes by Low Temperature Steam Annealing. *Energy Environ. Sci.* **2014**, *7*, 4044-4052.
- (22) Sowers, K.L.; Fillinger, A. Crystal Face Dependence of p-Cu₂O Stability as Photocathode. *J. Electrochem. Soc.* **2009**, *156*, F80-F85.
- (23) Zheng, Z.; Huang, B.; Wang, Z.; Guo, M.; Qin, X.; Zhang, X.; Wang, P.; Dai, Y. Crystal Faces of Cu₂O and Their Stability in Photocatalytic Reactions. *J. Phys. Chem. C* **2009**, *113*, 14448-14453.
- (24) Kwon, Y.; Soon, A.; Han, H.; Lee, H. Shape Effects of Cuprous Oxide Particles on Stability in Water and Photocatalytic Water Splitting. *J. Mater. Chem. A* **2015**, *3*, 156-162.
- (25) Huang, Q.; Kang, F.; Liu, H.; Li, Q.; Xiao, X. Highly Aligned Cu₂O/CuO/TiO₂ Core/shell Nanowire Arrays as Photocathodes for Water Photoelectrolysis. *J. Mater. Chem. A* **2013**, *1*, 2418-2425.
- (26) Jin, J.; Walczak, K.; Singh, M.R.; Karp, C.; Lewis, N.S.; Xiang, C. An Experimental and Modeling/Simulation-based Evaluation of the Efficiency and Operational Performance Characteristics of an Integrated, Membrane-free, Neutral pH Solar-Driven Water-Splitting

- system. *Energy Environ. Sci.* **2014**, *7*, 3371-3380.
- (27) Singh, M.R.; Papadantonakis, K.; Xiang, C.; Lewis, N.S. An Electrochemical Engineering Assessment of the Operational Conditions and Constraints for Solar-Driven Water-Splitting Systems at Near-neutral pH. *Energy Environ. Sci.* **2015**, *8*, 2760-2767.
- (28) Pourbaix, M. *Atlas of Electrochemical Equilibria in Aqueous Solutions*; Pergamon Press Ltd.: London, **1966**.
- (29) De Jongh, P.E.; Vanmaekelbergh, D.; Kelly, J.J. Cu₂O: a Catalyst for the Photoelectrochemical Decomposition of Water? *Chem. Commun.* **1999**, *12*, 1069-1070.
- (30) Dai, H.; Thai, C.K.; Sarikaya, M.; Baneyx, F.; Schwartz, D.T. Through-Mask Anodic Patterning of Copper Surfaces and Film Stability in Biological Media. *Langmuir* **2004**, *20*, 3483-3486.
- (31) Sinapi, F.; Lejeune, I.; Delhalle, J.; Mekhalif, Z. Comparative Protective Abilities of Organothiols SAM Coatings Applied to Copper Dissolution in Aqueous Environments. *Electrochim. Acta* **2007**, *52*, 5182-5190.
- (32) See, E.M.; Tossi, C.; Hällström, L.; Tittonen, I. Photodeposition of RuO_x Nanostructures on TiO₂ Films with a Controllable Morphology. *ACS Omega* **2020**, *5*, 10671-10679.
- (33) Yamamoto, M.; Minoura, Y.; Akasuka, M.; Ogawa, S.; Yagi, S.; Yamamoto, A.; Yoshida, H.; Yoshida, T. Comparison of Platinum Photodeposition Process on Two Types of Titanium Dioxide Photocatalysts. *Phys. Chem. Chem. Phys.* **2020**, *22*, 8730-8738.
- (34) Luo, Y.R. *Comprehensive Handbook of Chemical Bond Energies*; CRC Press: Boca Raton, FL, **2007**.
- (35) Sepahvandi, A.; Moztafzadeh, F.; Mozafari, M.; Ghaffari, M.; Raei, N. Photoluminescence in the Characterization and Early Detection of Biomimetic Bone-like Apatite Formation on the Surface of Alkaline-treated Titanium Implant: State of the Art. *Colloids Surf. B* **2011**, *86*, 390-396.
- (36) Prusi, A.R.; Arsov, L.D. The Growth Kinetics and Optical Properties of Films Formed under Open Circuit Conditions on a Titanium Surface in Potassium Hydroxide Solutions. *Corros. Sci.* **1992**, *33*, 153-164.
- (37) Zhang, L.; Zhang, J.; Dai, F.; Han, Y. Cytocompatibility and Antibacterial Activity of Nanostructured H₂TiO₅O₁₁·H₂O Outlayered Zn-doped TiO₂ Coatings on Ti for Percutaneous Implants. *Sci. Rep.* **2017**, *7*, 13951.
- (38) Zhang, K.; Zhang, T.; Wang, F.; Yuan, Y.; Li, Y. Exploration on Chemical Mechanical Planarization of ZnO Functional Thin Films for Novel Devices. *Microelectron. Eng.* **2013**, *101*, 37-41.
- (39) Mei, B.; Pedersen, T.; Malacrida, P.; Bae, D.; Frydendal, R.; Hansen, O.; Vesborg, P.C.K.; Serger, B.; Chorkendorff, I. Crystalline TiO₂: A Generic and Effective Electron-Conducting Protection Layer for Photoanodes and -Cathodes. *J. Phys. Chem. C* **2015**, *119*, 10519-10527.
- (40) Fitzgibbons, E.T.; Sladek, K.J.; Hartwig, W.H. TiO₂ Film Properties as a Function of Processing Temperature. *J. Electrochem. Soc.* **1972**, *119*, 735-739.
- (41) Nishikawa, M.; Fukuda, M.; Nakabayashi, Y.; Saito, N.; Ogawa, N.; Nakajima, T.; Shinoda, K.; Tsuchiya, T.; Nosaka, Y. A Method to Give Chemically Stabilities of Photoelectrodes for Water Splitting: Compositing of a Highly Crystallized TiO₂ layer on a Chemically Unstable Cu₂O Photocathode Using Laser-induced Crystallization Process. *Appl. Surf. Sci.* **2016**, *363*,

173-180.

(42) Wi, J.-H.; Kim, T.G.; Kim, J.W.; Lee, W.-J.; Cho, D.-H.; Han, W.S.; Chung, Y.-D. Photovoltaic Performance and Interface Behaviors of Cu(In,Ga)Se₂ Solar Cells with a Sputtered-Zn(O,S) Buffer Layer by High-Temperature Annealing. *ACS Appl. Mater. Interfaces* **2015**, *7*, 17425-17432.

(43) Liu, R.; Zheng, Z.; Spurgeon, J.; Yang, X. Enhanced Photoelectrochemical Water-Splitting Performance of Semiconductors by Surface Passivation Layers. *Energy Environ. Sci.* **2014**, *7*, 2504-2517.

Table of Contents

